CHALMERS
UNIVERSITY OF TECHNOLOGY

Radial discharge high shear homogenization and ultrasonication assisted pH-shift processing of herring co-products with antioxidant-rich materials

Food Chemistry 400 (2023) 133986

Contents lists available at ScienceDirect

Food Chemistry

journal homepage: www.elsevier.com/locate/foodchem

Radial discharge high shear homogenization and ultrasonication assisted pH-shift processing of herring co-products with antioxidant-rich materials for maximum protein yield and functionality

Jingnan Zhang [a,*], Anna Ström [b], Romain Bordes [b], Marie Alminger [a], Ingrid Undeland [a], Mehdi Abdollahi [a]

[a] Department of Biology and Biological Engineering-Food and Nutrition Science, Chalmers University of Technology, SE 412 96 Gothenburg, Sweden
[b] Department of Chemistry and Chemical Engineering-Applied Chemistry, Chalmers University of Technology, SE 412 96 Gothenburg, Sweden

ARTICLE INFO

Keywords:
Ultrasound
Protein ingredient
Fish
Cross-processing
Lipid oxidation
Natural antioxidant

ABSTRACT

Cross-processing herring co-products with antioxidant-rich helpers including lingonberry-press-cake, shrimp-shells and seaweed was reported to mitigate lipid oxidation but reduce protein yield. Here, four strategies were used to counteract such yield-reduction; optimizing solubilization/precipitation pH, increasing raw-material-to-water-ratio, replacing single-stage-toothed- by radial-discharge- high-shear-mechanical-homogenization (RD-HSMH) and ultrasonication (US). The effects of RD-HSMH and US on lipid oxidation, protein structural and functional properties were studied. Combining four strategies improved total protein yield by 5–12 %, depending on helper type. More than the confirmed antioxidant effects, cross-processing also improved protein water solubility and emulsification activity but reduced gelation properties. RD-HSMH generally improved protein emulsifying and gelation properties but reduced protein water solubility. US reduced protein water solubility and gelation properties. Altogether, it was recommended for all helpers to increase solubilization pH to 12 and raw-material-to-water-ratio to 1:6 followed by RD-HSMH at 8000 rpm for 90 s, aiming for maximum protein yield and emulsifying and gelation properties.

1. Introduction

Herring (*Clupea harengus*) is a small dark muscle-rich fish that yielded 1820 thousand tons of live weight of capture production in 2018, which was the fourth-highest among all finfish species (FAO, 2020). Herring is valuable for human consumption as a rich source of high-quality protein, long-chained n-3 polyunsaturated fatty acids (LC n-3 PUFAs), vitamin D, calcium, selenium, and iodine (Larsen, Eilertsen, & Elvevoll, 2011), but still, large amounts of the catch leave the food chain and become feed for e.g. fur animals or fish. Primarily, it is small herring (<55 g), and herring co-products that are used for this purpose. Filleting of herring yields ~ 60 % co-products including heads, backbones, tails, and viscera (Abdollahi & Undeland, 2018). Herring heads and backbones, which account for > 75 % of these co-products, are rich in muscle and therefore potential sources of high-quality functional proteins. However, their isolation is rendered difficult based of the abundance of PUFA, prooxidants, and impurities such as bones, scales, connective tissues, and pigments. These constituents result in rancidity, low protein yield and poor color when conventional protein concentrating processes such as mechanical meat/bone separation, with and without subsequent washing, are applied to herring or other fish co-products (Kristinsson & Liang, 2006; Wu, Abdollahi, & Undeland, 2021).

The pH-shift processing allows a more selective separation of fish proteins from complex raw materials compared to mechanical separation. This technique has shown high protein recoveries from e.g. gutted fish (Abdollahi, Rezaei, Jafarpour, & Undeland, 2019; Marmon & Undeland, 2010) and fish processing co-products (Chomnawang & Yongsawatdigul, 2013; Hinchcliffe, Carlsson, Jönsson, Sundell, & Undeland, 2019; Pramono, Pujiastuti, & Sahidu, 2018). However, during pH-shift processing of herring-derived raw materials, lipid oxidation has been reported to be a problem due to the mentioned abundance of PUFA and heme proteins even though the pH-shift method can remove large amounts of both lipids and heme proteins, the remaining levels are still enough to cause lipid oxidation during the actual processing step

* Corresponding author.
E-mail addresses: jingnan.zhang@chalmers.se (J. Zhang), anna.strom@chalmers.se (A. Ström), bordes@chalmers.se (R. Bordes), marie.alminger@chalmers.se (M. Alminger), undeland@chalmers.se (I. Undeland), khozaghi@chalmers.se (M. Abdollahi).

https://doi.org/10.1016/j.foodchem.2022.133986
Received 21 March 2022; Received in revised form 27 July 2022; Accepted 18 August 2022
Available online 23 August 2022

and the subsequent storage of protein isolates (Undeland et al., 2005; Wu et al., 2021). Our research group has recently proven that cross-processing herring co-products with raw materials rich in natural antioxidants, such as seaweed or agricultural as well as shellfish side streams (referred to as "helpers") can be a new approach to minimize lipid oxidation both during and after pH-shift processing (Abdollahi, Olofsson, Zhang, Alminger, & Undeland, 2020; Zhang, Abdollahi, Alminger, & Undeland, 2022). However, the cross-processing significantly lowered protein yields compared to classic pH-shift processing of herring co-products (Abdollahi et al., 2020). Considering the nature of the interactions of the helpers with the fish co-products, we here hypothesized that tuning the pH-shift process and/or applying assistant technologies are necessary to optimize the process to these combinations of raw materials. This approach has not previously been evaluated.

In previous studies, it has been found that the exact solubilization and precipitation pH's for proteins in the pH-shift process are species-dependent. Most studies have shown herring proteins in 6–9 volumes of water had maximum solubility between pH 11.2–12.5 (alkali-aided solubilization) and pH 2–2.7 (acid-aided solubilization); and maximum perceptibility between pH 5.4–6.1 (Abdollahi & Undeland, 2018; Hinchcliffe et al., 2019; Marmon & Undeland, 2010). However, when introducing plant-, shellfish- or seaweed raw materials (Abdollahi et al., 2020), protein solubilization at pH 11.5 and precipitation at pH 5.5 were reduced to different extents, possibly as a result of polyphenol-protein crosslinks, competition for water between proteins and other macromolecules e.g. polysaccharides, or changed surface charges due to the introduction of salt (from seaweed). Whether these features could be counteracted by increasing the amount of water or altering solubilization and/or pH of precipitation has so far not been reported.

High shear mechanical homogenization (HSMH) is a common and affordable technology to assist the conversion of solid/semi-solid materials like bones, muscle or plant tissue to a liquid or slurry (Zhou et al., 2019), thus, often constituting the first step in extraction protocols. During HSMH, a high-speed rotational cutter creates a flow of materials that generates strong, turbulent and cavitation effects that allow the mixture to be homogenized quickly and evenly (Zhou et al., 2019). However, depending on the design of the inner and external cutters installed on the head of the homogenizer, strong shear forces will be generated between the cutters (e.g. single-stage toothed (SST) high shear homogenizer) or the larger particles will continuously pass through small holes (e.g. radial discharge (RD) high shear homogenizer) gradually dispersing them into finer particles (Zhou et al., 2019). Hereby, the high rotation speed in combination with the high-intensity shear force, fierce collision, pressure differential relief and other forces substantially promotes extraction of compounds from the homogenized material into a liquid system (Zhou et al., 2019).

Ultrasonication (US) has also shown great potential in improving the outcomes of the pH-shift processing of aquatic raw materials such as tilapia (*Oreochromis niloticus*) fillets (Tian, Wang, Zhu, Zeng, & Xin, 2015) and whole mackerel (*Scomber scombrus*) (Alvarez et al., 2018) since it is a non-thermal technology. Acoustic cavitation and microstreaming induced by US can not only promote extraction efficiency but also modify protein functionality (Soria & Villamiel, 2010). Cavitation generates turbulence, high-velocity inter-particle collisions and micropores. This improves the permeation of the solvent into the matrix, promoting the interaction between target compounds and solvent, thus, enhancing the extraction efficiency (Das, Goud, & Das, 2017). In addition, microstreaming leads to a relative movement between the solvent and polymer molecules, inducing shear forces which ultimately also increase the extraction efficiency by accelerating mass transfer and internal diffusion mechanisms. However, the risk for conformational protein changes induced by the destruction of covalent bonds, hydrogen bonds and electrostatic forces through cavitation effects must be carefully controlled since such changes may affect the protein functionality. To the best of our knowledge, neither the effect of different HSMH principles nor US treatment on protein yield and functionality during joint pH-shift processing of fish and non-fish raw materials has been studied, but their inclusion in such cross-processing approaches could be a route to optimized yields.

The present study was aimed at maximizing protein yield during cross-processing of herring co-products with lingonberry press-cake, shrimp shells and green seaweed by tuning solubilization and precipitation pH's, increasing the water ratio and by introducing more powerful HSMH as well as US treatment. The impacts of HSMH and US treatments on lipid oxidation during the process, and on the structural and functional properties of the cross-processed protein isolates were also studied.

2. Materials and methods

2.1. Chemicals and reagents

Sodium chloride, sodium carbonate, hydrochloric acid, trichloroacetic acid, acetic acid, sodium dodecyl sulphate, ethylenediaminetetraacetic acid, 1,1,3,3-Tetramethoxypropane, butylated hydroxytoluene, urea, glycine, Ellman's reagent (5,5′-Dithiobis-(2-nitrobenzoic acid)), copper(II) sulfate pentahydrate, dichloromethane and Folin & Ciocalteu's phenol reagent (2 N) were from Sigma-Aldrich Co. (USA). 2,4-Dinitrophenylhydrazine was from Sigma-Aldrich Co. (India). 8-Anilinonaphthalene-1-sulfonic acid was from Sigma-Aldrich Co. (Switzerland). Sodium hydroxide and methanol were from Honeywell Riedel-de Haën AG (Germany). Chloroform was from VWR Chemicals BDH (USA). Sulfuric acid was from Merck (USA). Potassium sodium tartrate tetrahydrate was from Thermo Scientific (Spain). Tris (hydroxymethyl) aminomethane was from Acros Organics (Germany). All chemicals used were reagent grade.

2.2. Preparation of marine and agricultural materials

Herring (*Clupea harengus*) filleting co-products including heads and backbones were provided by *Sweden Pelagic AB* (Ellös, Sweden). The fresh co-products were directly transported to Chalmers University of Technology on ice and ground in a tabletop meat grinder with a 4.5 mm hole plate (C/E22 N, Minerva Omega Group, Italy). The minced co-products were stored at −80 °C until use. Lingonberry (*Vaccinum vitis-idaea*) press-cake from industrial juice production provided by *Grangärde Musteri AB* (Dalarna, Sweden) was transported to Chalmers University of Technology in November 2019 after being stored at −20 °C for five months. Lingonberry press-cake contained peels, seeds, leaves, stems and leftover flesh. On a wet weight basis, the amounts of leaves and seeds were 9 % and 24 %, respectively. Shrimp shells including cephalothorax, legs, peels and tails emerging as a by-product during industrial steaming and peeling of shrimps were provided by *Räkor-och Laxgrossisten AB* (Gothenburg, Sweden). Shrimp shells were sent to Chalmers University of Technology in March 2018 after being stored at −25 °C for three months. The tank-cultivated green seaweed (*Ulva fenestrata*) was provided by *Sven Lovén Centre for Marine Infrastructure* (Tjärnö, Sweden), which was harvested in November 2019 and transported on ice within a day after harvesting. Lingonberry press-cake, shrimp shells and green seaweed were ground similarly to fish co-products and stored at −80 °C until use.

2.3. Basic protocol for production of cross-processed protein isolates at optimal solubilization/precipitation pH's

The minced herring co-products and helpers were thawed by cold running water. For herring controls, i.e., without helpers, herring co-products were mixed with ice-cold distilled water at a ratio of 1:6 on a wet weight basis. When inducing helpers, green seaweed was pre-treated by osmo-shocking for 15 min, while lingonberry press-cake and shrimp shells were directly added to herring co-products in an amount that corresponded to 30 % of herring co-products' dry weights

(see **supplementary** Table 1 for moisture content of raw materials). The amount of herring co-products, helper and distilled water, as well as the initial pH of herring co-products without or with (wo/w) the addition of helper are presented in Table 1. Ice-cold distilled water was then added to the combined raw materials to obtain the same dry weight to moisture ratio as the herring controls, followed by high shear mechanical homogenization (HSMH) with a single-stage toothed (SST) homogenizer (T18 digital Ultra-Turrax homogenizer, IKA, Germany) at 10,000 rpm for 1 min (this treatment hereafter referred to as SST-HSMH). The pH of homogenate was adjusted by 2 M NaOH to the optimal solubilization pH, which was pH 12 for all samples based on information on protein solubility as a function of pH (see **section 2.4**). The pH-adjusted homogenates (H) were then incubated on ice for 10 min and centrifuged (8,500 × g, 20 min, 4 °C). The supernatants (S1) were separated from the floating layer and sediments by a sieve. H and S1 samples were collected to determine protein solubility and solubilization yield by using Equation (1)-(2). During the precipitation step, 2 M HCl was added to S1 to achieve the optimum precipitation pH's for different samples: 5.5 for herring controls; 5.0 for the combinations with lingonberry presscake or shrimp shells; 4.5 for the combination with green seaweed. Then, the pH-adjusted S1 was incubated on ice and centrifuged, according to the above. The supernatant (S2) was then removed from the precipitated protein pellet (i.e., protein isolates) and sampled. Protein precipitation yield and total yield were calculated by Equation (3)-(4). Protein isolates were collected, manually stirred on ice to even out ingradients and stored at −80 °C. All samples were placed on ice throughout the process.

$$Solubility\,(\%) = \frac{c_{S1}}{c_H} \times 100 \quad (1)$$

$$Solubilization\ yield\,(\%) = \frac{c_{S1} \times V_{S1}}{c_{H\times} V_H} \times 100 \quad (2)$$

$$Precipitation\ yield\,(\%) = \frac{c_{S1} \times V_{S1} - c_{S2} \times V_{S2}}{c_{S1} \times V_{S1}} \times 100 \quad (3)$$

$$Total\ yield\,(\%) = \frac{c_{S1} \times V_{S1} - c_{S2} \times V_{S2}}{c_{H\times} V_H} \times 100 \quad (4)$$

where, V_x is the volume of homogenate (H) and supernatants (S1 and S2); c_x is protein concentration in homogenate (H) and in supernatants (S1 and S2), which was measured by a modified version of Lowry protein assay (Markwell, Haas, Bieber, & Tolbert, 1978) based on the reaction of copper ions produced by the oxidation of peptide bonds, with Folin-Ciocalteu reagent. The resulted blue color was measured by absorbance at 660 nm. Bovine serum albumin (99 %, Sigma-Aldrich Co., Germany) was used as the standard.

2.4. Evaluating protein solubility and solubilization yield as a function of pH

To optimize the solubilization and precipitation pH's for the pH-shift processing of herring co-products wo/w helpers, protein solubility and solubilization yield as a function of pH were evaluated. The homogenates of raw materials were prepared as described in **Section 2.3**. The pH of the homogenate was then monitored and adjusted to acidic or alkaline conditions by drops of 2 M HCl or 2 M NaOH, respectively. At different pH's, 10 ml of pH-adjusted homogenate (H) was collected for protein content measurement; another 30 ml were collected, incubated on ice and centrifuged, according to **Section 2.3**, to obtain a supernatant (S1) containing solubilized proteins. All samples were placed on ice throughout the process. Protein solubility and solubilization yield were calculated by Equation (1)-(2).

2.5. Modifications of the basic cross-processing protocol for higher protein yield

2.5.1. Increasing the addition of water

The amount of water used in the basic protocol of cross-processing was adjusted to keep the same ratio of dry matter to moisture as the herring controls, as previously reported (Abdollahi et al., 2020). To evaluate the effect of water ratio on protein solubility and yield during

Table 1
The amount of helper added per 100 g herring co-products which corresponded to 30 % of herring co-products' dry weight; initial pH of herring co-products wo/w addition of helpers; protein solubility and protein yields determined during the cross-processing of herring co-products wo/w different helpers by using different water amounts, HSMH treatments and US. Data are shown as mean values ± standard deviation ($n_e \geq 2$, n ≥ 2). SST = Single-stage toothed, RD = Radial discharge.

Source	Helper (g)	Initial pH	Water addition		Treatment**	Protein solubility (%)	Protein yield (%)		
			Addition level*	Water (g)			Solubilization	Precipitation	Total
Herring co-products	–	6.7 ± 0.0	Basic	600	SST-HSMH	90.0 ± 0.1^{b}	81.2 ± 0.2^{ab}	95.5 ± 0.2^{a}	77.5 ± 0.3^{a}
					RD-HSMH	87.6 ± 0.6^{b}	76.9 ± 0.2^{cde}	93.7 ± 0.2^{bc}	72.0 ± 0.4^{b}
					RD-HSMH+US	90.2 ± 1.1^{b}	77.9 ± 1.2^{cd}	93.7 ± 0.2^{bc}	73.0 ± 1.2^{b}
Herring co-products +Lingonberry presscake	36	5.1 ± 0.2	Basic	775	SST-HSMH	73.1 ± 0.9^{f}	61.9 ± 0.9^{i}	94.5 ± 0.0^{b}	58.5 ± 0.9^{e}
			Increased	814	SST-HSMH	79.9 ± 1.7^{de}	66.6 ± 1.1^{h}	94.3 ± 0.2^{b}	62.8 ± 0.9^{d}
					RD-HSMH	80.2 ± 0.8^{de}	66.1 ± 0.8^{h}	93.8 ± 0.0^{bc}	62.0 ± 0.8^{d}
					RD-HSMH+US	88.0 ± 0.3^{b}	72.9 ± 0.8^{fg}	93.6 ± 0.1^{bcd}	68.2 ± 0.7^{c}
Herring co-products +Shrimp shells	90	8.2 ± 0.0	Basic	730	SST-HSMH	78.4 ± 0.2^{e}	61.6 ± 0.3^{i}	91.0 ± 0.2^{g}	56.1 ± 0.2^{e}
			Increased	1138	SST-HSMH	82.2 ± 0.1^{cd}	71.3 ± 0.4^{g}	92.6 ± 0.7^{def}	66.1 ± 0.1^{c}
					RD-HSMH	89.8 ± 1.2^{b}	78.9 ± 1.7^{bc}	93.7 ± 0.7^{bc}	73.9 ± 1.1^{b}
					RD-HSMH+US	83.1 ± 1.5^{c}	73.8 ± 0.7^{efg}	91.3 ± 0.4^{g}	67.4 ± 0.9^{c}
Herring co-products +Green seaweed	48	6.5 ± 0.2	Basic	762	SST-HSMH	78.6 ± 0.0^{e}	56.4 ± 0.6^{j}	92.5 ± 0.2^{ef}	52.1 ± 0.7^{f}
			Increased	889	SST-HSMH	89.3 ± 1.6^{b}	74.9 ± 0.8^{def}	91.8 ± 0.2^{fg}	68.8 ± 0.9^{c}
					RD-HSMH	94.5 ± 0.2^{a}	77.3 ± 2.4^{cd}	93.0 ± 0.2^{cde}	71.9 ± 2.4^{b}
					RD-HSMH+US	95.0 ± 0.1^{a}	83.2 ± 0.4^{a}	92.4 ± 0.3^{ef}	76.9 ± 0.6^{a}

Different small letters in each column show a significant difference ($p < 0.05$).
*Basic water addition was to obtain the same dry weight to moisture ratio as for the herring controls (w/w); increased water addition was equaled to six times of the total wet weight of raw materials.
**SST-HSMH and RD-HSMH imply raw materials were treated by a SST homogenizer at 10,000 rpm for 60 s, or by a RD homogenizer at 8,000 rpm for 90 s. RD-HSMH was more efficient than SST-HSMH in dispersing raw materials. US was applied to pH-adjusted homogenates during the protein solubilization step.

cross-processing, the amount of water was increased to six times the raw materials' wet weights. A summary of the water addition used in each combination of raw materials is presented in Table 1. The other processing steps were conducted according to the above.

2.5.2. More efficient HSMH

The SST homogenizer was replaced by radial discharge (RD) high shear homogenizer (L5M-A, Silverson, UK) to subject raw materials to HSMH at 8,000 rpm for 90 s, this treatment hereafter referred to as RD-HSMH. The effects of RD-HSMH on protein yield and protein isolate quality were compared to the results obtained with SST-HSMH (see **section 2.3**). The other processing steps were conducted as before.

2.5.3. Ultrasonication (US) assisted cross-processing

A combination of cross-processing and US was conducted by subjecting the homogenate, right after adjusting its pH to the optimum solubilization pH found in **section 2.3**, to sonication with an US probe (Sonifier 250, Branson, USA). The output control which controls the amplitude i.e., peak to peak motion, of the ultrasonic vibrations, was 6.5, and the duty cycle was 90 % (ultrasonics on for 90 % of every second). Homogenates were placed on the ice during the treatment. The probe was put at the bottom of homogenates for 2 min, then after 1 min pause to limit temperature rise, for another 2 min in the middle. The other processing steps were conducted as before.

2.6. Analysis of lipid oxidation-derived aldehydes formed during processing

Malondialdehyde (MDA) and 4-hydroxy-(E)-2-hexenal (HHE) contents of herring co-products, helpers and protein isolates were measured. Helpers were analyzed to avoid interference. Herring co-products, helpers and protein isolates were thawed under cold running water. Different amount of ice-cold Milli Q water was added to equalize the moisture content of protein isolates to the same as the isolate having the highest moisture content (83.4 %). Three grams of herring co-products and helpers were mixed with an equal amount of ice-cold Milli Q water while the 3 g of protein isolates were diluted with 9 ml of ice-cold Milli Q water. The mixtures were homogenized (T18 digital Ultra-Turrax, IKA, Germany) on ice at 20,000 rpm for 15 s (n = 2). Five hundred μl of homogenate was then transferred to a 1.5 ml Eppendorf tube containing 20 μl of BHT (0.45 M in MeOH) and 40 μl of EDTA (0.02 M in Milli Q) to prevent lipid oxidation during analysis. The contents of MDA and HHE were measured by the method explained by Tullberg et al. (2016) using DNPH-derivatization followed by LC–MS analysis. Standard curves of MDA and HHE were made in the range of 1–55 μM and 0.01–1 μM, respectively.

2.7. Characterization of cross-processed protein isolates

2.7.1. Proximate composition analysis

Crude protein content of the herring co-products, helpers and their corresponding protein isolates was measured by a modified version of the Dumas method reported by Marcó, Rubio, Compañó, and Casals (2002), using a LECO nitrogen analyzer (TruMac-N, LECO Corp., USA). The nitrogen-to-protein conversion factor used was 5.58 for herring co-products and protein isolates, 5.4 for lingonberry press-cake, 3.88 for shrimp shells and 5 for green seaweeds (Zhang et al., 2022). Crude lipid content was analyzed using a modified version (Zhang et al., 2022) of Lee's method. Ash content was determined by placing samples in a crucible and heating at 550 °C for 6 hrs.

2.7.2. Active and total sulfhydryl groups measurement

Active and total sulfhydryl groups were determined by a modified version of Ellman's method as described by Gong et al. (2015). One hundred and eighty milligrams of freeze-dried protein isolate powder was dissolved in 30 ml of tris–glycine buffer (0.086 M tris, 0.09 M glycine, 4 mM EDTA, pH 8.0) containing 8 M urea, followed by stirring for 30 min. The solution was centrifuged at 10,000×*g* for 10 min. The supernatant was collected, and its protein concentration was measured by Lowry method as described in 2.3. The content of active sulfhydryl groups was measured by adding 160 μl of Ellman's reagent (5,5′-Dithiobis-(2-nitrobenzoic acid), DTNB) (4 mg/mL in tris–glycine buffer) to 4 ml properly diluted supernatant, followed by 15 min of incubation before reading the absorbance at 412 nm. To measure the total sulfhydryl groups, 8 μl of 2-mercaptoethanol was added to 4 ml supernatant followed by incubation at 25 °C for 2 h before adding 10 ml 12 % trichloroacetic acid (TCA). After another hour of incubation at 25 °C, the solution was centrifuged at 10,000×*g* for 10 min. The pellet was washed with 5 ml 12 % TCA two more times and dissolved in 6 ml tris–glycine buffer. Four milliliters of properly diluted supernatant were mixed with 160 μl Ellman's reagent, incubated and read at 412 nm as described above. Ellman's reagent in tris–glycine buffer was used as the control. The content of active/total sulfhydryl groups was calculated by Equation (5).

$$Active/total\ sulfhydryl\ groups\,(\mu mol/g) = \frac{73.53 \times Abs \times DF}{c} \quad (5)$$

where *Abs* is the absorbance at 412 nm, *DF* is the dilution factor and *c* is the sample concentration (mg protein/ml).

2.7.3. Surface hydrophobicity analysis

Surface hydrophobicity of protein isolates was measured by a modified version of Kato's method as described by Timilsena, Adhikari, Barrow, and Adhikari (2016). Forty milligrams of freeze-dried protein isolate powder were dissolved in 40 ml of phosphate buffer (0.01 M, pH 7.0) and vortexed for 1 min, followed by centrifugation (10,000×*g*, 20 min) to remove insoluble fractions. The supernatant was collected, and its protein concentration was measured by Lowry method as described in 2.3. The supernatant was diluted serially by phosphate buffer. The surface hydrophobicity was determined by adding 20 μl of 8-Anilinonaphthalene-1-sulfonic acid (ANS) solution (8 mM in phosphate buffer) to 4 ml diluted solutions. After incubating in darkness for 15 min, the fluorescence intensity of ANS-protein conjugates was measured by using excitation and emission wavelengths of 374 and 485 nm, respectively. ANS solution and diluted supernatants were used as controls. The net intensity was plotted against the protein content (%). The slope as determined by linear regression was considered as an index of average protein surface hydrophobicity.

2.7.4. Sodium dodecyl sulfate–polyacrylamide gel electrophoresis (SDS-PAGE)

Laemmi's method for SDS-PAGE modified by Abdollahi and Undeland (2018) was used to analyze the polypeptide pattern of herring co-products, helpers, and protein isolates. Two grams of each sample were mixed with 18 ml of 5 % sodium dodecyl sulphate (SDS) solution. The protein concentration of sample solution was measured by Lowry method as described in **section 2.3** and adjusted to 4 μg protein/μl by 5 % SDS. Fifty microliters of diluted sample solutions were mixed with an equal amount of Laemmli buffer (Bio-Rad, USA) containing 5 % β-mercaptoethanol (Bio-Rad, USA), followed by heating at 95 °C for 5 min by a heater block. Five microliters of the ladder (Prestained dual-color standard, 10– 250 kDa, Bio-Rad, USA) and 20 μl sample solutions were loaded onto a precast mini linear gel 4–20 % (Bio-Rad, USA). Electrophoresis was conducted at a constant voltage of 125 V, using a Mini Protein II unit (Bio-Rad, USA). After separation, 0.02 % (w/v) Coomassie Brilliant Blue R-250 (Bio-Rad, USA) in 50 % (v/v) methanol and 7.5 % (v/v) acetic acid was used for staining, followed by destaining using 50 %methanol (v/ v) and 7.5 % (v/v) acetic acid for 40 min. The gel was scanned in the GelDoc Go Imaging System (Bio-Rad, USA) after storing in the fridge overnight.

2.7.5. Determination of protein water solubility

One gram of each freeze-dried protein isolate was dissolved in 40 ml distilled water and vortexed for 90 s to obtain protein solutions. The pH of the solution was adjusted to 7 or 11 by 2 M NaOH, followed by centrifugation at 15,000×*g* for 30 min at 4 °C. Protein water solubility (%) was determined by Equation (6).

$$Protein\ water\ solubility\ (\%) = \frac{c_{after}}{c_{before}} \times 100 \quad (6)$$

where, c_x is protein concentration in protein solution before centrifugation (c_{before}) and in supernatant after centrifugation (c_{after}). Protein concentration was measured by Lowry method as described in 2.3.

2.7.6. Determination of emulsifying properties

Emulsifying activity index (EAI) and emulsion stability index (ESI) of the protein isolates were measured according to the method explained by Ogunwolu, Henshaw, Mock, Santros, and Awonorin (2009). Three hundred milligrams of each freeze-dried protein isolate were dispersed in 30 g of distilled water and vortexed for 1 min, followed by the addition of 10 g sunflower oil. The pH of the mixture was adjusted to 3, 5, 7, 9, and 11 using 1 M HCl and 1 M NaOH. Oil-in-water emulsion was then prepared by homogenizing the mixture at 20,000 rpm for 1 min. Fifty microliters of the aliquot of the emulsion were transferred to 5 ml of 0.1 % of SDS solution immediately and after 10 min, followed by vortexing for 20 s. The absorbance of the solution was measured at 500 nm. The EAI and ESI were calculated using Equation (7) and Equation (8), respectively (Pearce & Kinsella, 1978).

$$EAI\ (m^2/g) = \frac{2 \times 2.303 \times Abs_0 \times DF}{c \times \varphi \times \theta \times 10000} \quad (7)$$

$$ESI\ (min) = \frac{Abs_{10} \times \Delta t}{\Delta Abs} \quad (8)$$

where, Abs_x is the absorbance at 500 nm, DF is the dilution factor used when measuring Abs_0, c is the initial concentration of protein (g/ml), φ is the oil volume fraction in the emulsion, which is 0.25, θ is the path length of the cuvette (1 cm), Δt is the elapsed time (10 min), $\Delta Abs = Abs_0 - Abs_{10}$.

2.7.7. Evolution of storage moduli of the protein isolates

The evolution of storage moduli (G') of protein isolates were analyzed using a dynamic rheometer (Paar Physica Rheometer MCR 300, Anton Paar GmbH, Austria) with a parallel-plate geometry (25 mm diameter). The gap between the plates was set at 1 mm. Protein isolates were thawed under running tap water. Then, the moisture content of the protein isolates was equalized to 80 % by adding ice-cold distilled water if needed, and 2 % (w/w) NaCl was added to the samples which were thereafter chopped on ice for 1.5 min using a mini chopper to obtain a homogeneous paste. Then, 2 g of the paste was loaded to the rheometer and pressed by the upper plate by lowering it to the measurement position (1 mm gap). The excess sample was removed, and the exposed sample was covered by mineral oil to prevent evaporation during the analysis. The storage modulus were recorded during a temperature increase from 20 °C to 90 °C at a heating rate of 1 °C/min followed by an isothermal step (90 °C, 30 min) and finally a cooling step from 90 °C to 20 °C (rate: 1 °C/min). The temperature sweep was conducted at a 1 % strain and 0.1 Hz frequency.

2.7.8. Gel preparation and puncture test of the gels

The pastes were prepared in the same manner as for rheological analysis. The homogeneous paste was loaded into a plastic tube with 18 mm diameter, which had both ends sealed tightly. The paste was subjected to a two-step cooking by setting at 35 °C in a water bath for 30 min, followed by 20 min of cooking at 90 °C to form a gel. The gels were cooled down immediately in a water–ice slurry for 30 s to avoid further heating. The gels were stored at 4 °C overnight before analysis.

Puncture tests of the gels were conducted by using a texture analyzer (TVT 6700, Perten Instruments, Australia) equipped with a 5-kg load cell. After equilibration at room temperature for 1 h, gel cylinders with a length of 20 mm were prepared. A puncture test was then conducted on the gels with a 5-mm spherical probe, at a depression speed of 1 mm/*sec*. Penetration force and the distance of the probe entered the gel were recorded.

2.8. Statistical analysis

All pH-shift process experiments (e) with different herring co-product + helper combinations were carried out at least in duplicates (i.e., $n_e \geq 2$) and analyses of protein yield or protein isolate characteristics from each experiment were also carried out at least in duplicates (i.e., $n \geq 2$). Significant differences between sample groups regarding the different parameters were analyzed by one-way analysis of variance (ANOVA) followed by Duncan's multiple range test by using SPSS software (IBM SPSS Statistics Version 24, IBM Inc., Chicago). The significance level (p) was set at 0.05, below which the differences were considered significant.

3. Results and discussion

3.1. Protein solubility and yield

3.1.1. Protein solubility and solubilization yield as a function of pH

To find optimal solubilization and precipitation pH's to be used when cross-processing herring co-products with different helpers, protein solubility and solubilization yield as a function of pH were studied. As shown in Fig. 1, protein solubility and solubilization yield showed "U-shaped" curves for all samples. For herring controls, i.e. without helpers, the lowest protein solubility and solubilization yield were found at pH 5.5 and reached their maximum values at extreme acidic and alkaline environments, which was in agreement with previous studies (Abdollahi & Undeland, 2018; Geirsdottir, Hlynsdottir, Thorkelsson, & Sigurgisladottir, 2007). When inducing helpers, protein solubility and solubilization yield were reduced, which was consistent with our earlier findings (Abdollahi et al., 2020). This could be related to co-precipitation of proteins with phenolic compounds and polysaccharides brought by lingonberry press-cake and green seaweed (Czubinski & Dwiecki, 2017; Dhouafli et al., 2018); or the presence of calcium carbonate inducing coagulation and precipitation of proteins when adding shrimp shells (Polowczyk, Bastrzyk, & Fiedot, 2016). The results also illustrated that the combination of herring co-products and lingonberry press-cake provided high protein solubility and solubilization yield at both acidic and alkaline environments, while the addition of shrimp shells or green seaweed dramatically decreased protein solubility and yield under acidic conditions. The extremely low protein solubility and solubilization yield in presence of green seaweed could be related to competition for water between the seaweed-derived polysaccharides and herring proteins, given the high water holding capacity of the former. The low solubility of green seaweed proteins themselves at low pH's caused e.g., by its high ionic strength could also be a contributing factor. Thus, it can be inferred that while both acid- and alkali-aided solubilization were suitable for cross-processing herring co-products with lingonberry press-cake, only alkali-aided solubilization was compatible in presence of shrimp shells or green seaweed. For all three helpers, results also revealed that the solubilization pH should be increased from the previously used 11.5 (Abdollahi et al., 2020) to 12, while the precipitation pH should be decreased from previously used 5.5 (Abdollahi et al., 2020) to 5.0 or 4.5 during alkali-aided solubilization to compensate for the loss of protein solubility and yield caused by the helpers.

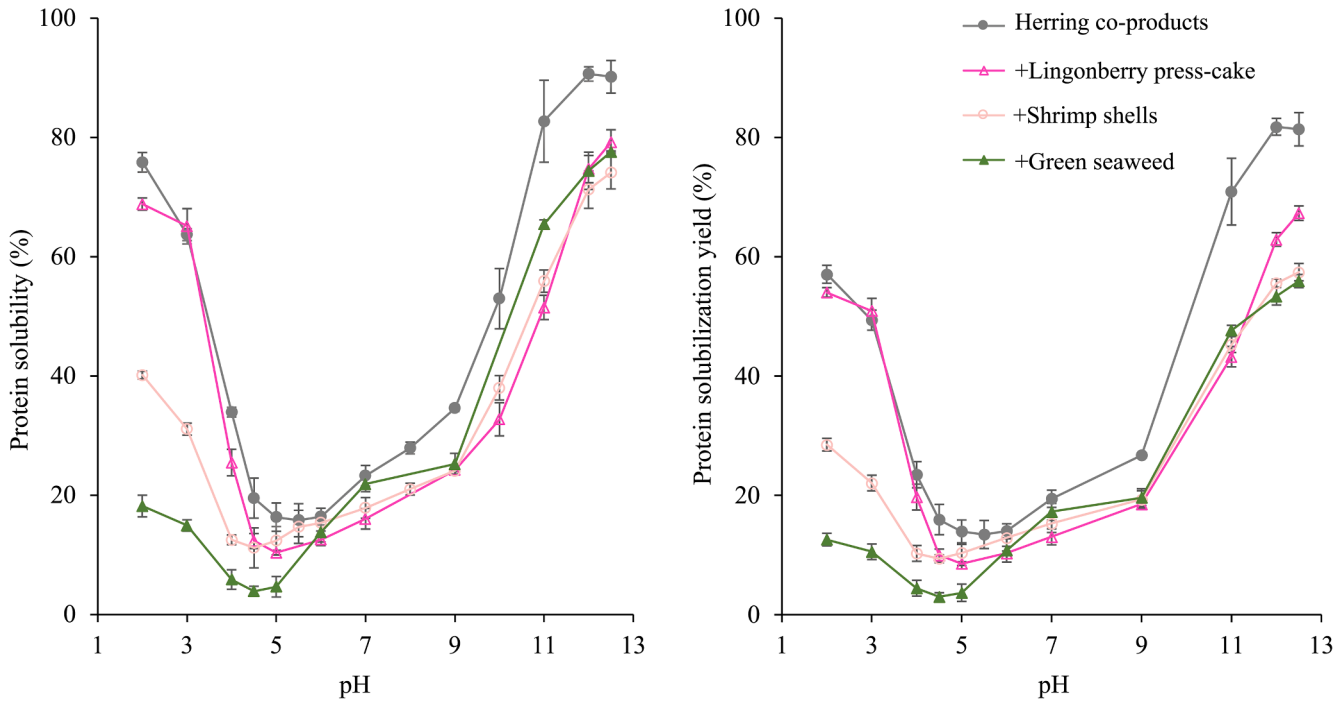

Fig. 1. Protein solubility (A) and solubilization yield (B) as a function of pH for herring co-products alone and its combinations with lingonberry press-cake, shrimp shells and green seaweed.

3.1.2. Protein solubility and total yield as a function of water amount, HSMH principle and US

Table 1 summarizes protein solubility and yields obtained during alkali-aided pH-shift processing of herring co-products without/with (wo/w) different helpers. The amount of water used for the basic cross-processing protocol provided the same ratio of moisture to dry matter (w/w) as for the herring controls (i.e. 600:29) (Abdollahi et al., 2020). Given the fact that some of the water provided by the raw materials themselves does not act as a solute, we hypothesized that there would not be enough water for efficient protein solubilization in all raw material combinations. To facilitate extractions of proteins from both herring co-products and helpers, the water amount was therefore increased to six times the weight of the combined raw materials' wet weights. The significantly ($p < 0.05$) improved protein solubility and yield during the solubilization step for all helpers are shown in Table 1, especially for green seaweed. To further increase yields up to those of herring controls, RD-HSMH, with and without US, were also added to the process protocols. Replacing SST-HSMH by RD-HSMH during the cross-processing of herring co-products with shrimp shells or green seaweed showed great improvement in protein solubilization, precipitation and total yields, to the same levels as for herring controls. These improvements could be related to the finer dispersion of raw materials generated by RD-HSMH as documented by visual observations, facilitating protein solubilization. In addition, the increased protein solubilization yield for the combination with green seaweed could be related to better extraction of seaweed protein, which was reflected by SDS-PAGE patterns of green-seaweed-derived protein isolates compared to herring protein isolates (see Fig. 2). This observation could be explained by that RD-HSMH was able to break down seaweed cell walls more efficiently (Postma et al., 2017). However, no significant improvement from RD-HSMH was found for the combination with lingonberry press-cake, indicating a need for other methods to compensate for the protein yield losses induced by lingonberry press-cake. The use of US, however, significantly ($p < 0.05$) increased solubilization yields and total yields

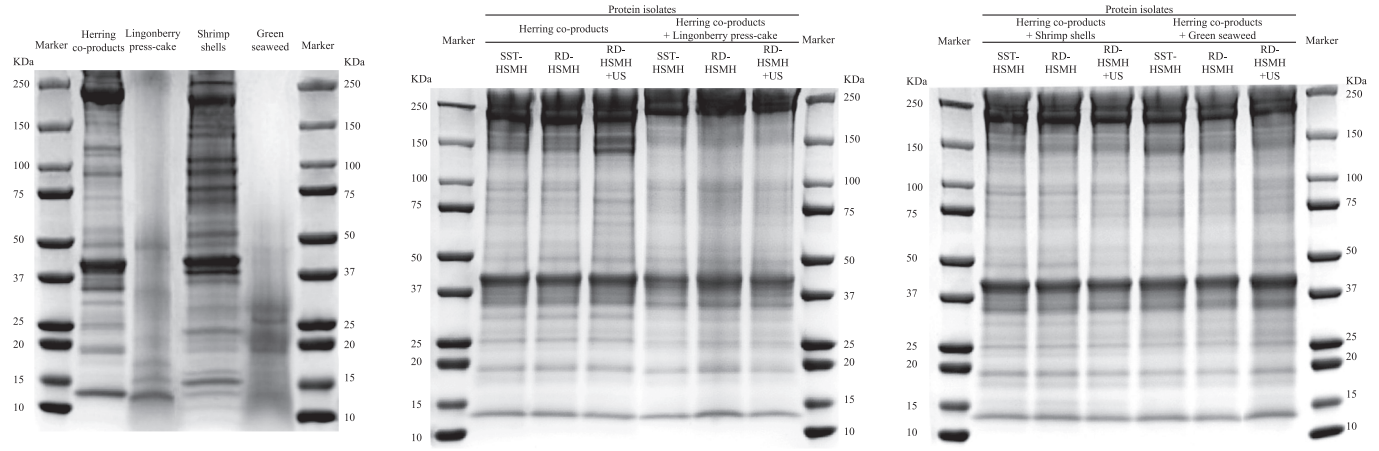

Fig. 2. SDS-PAGE patterns of herring co-products, lingonberry press-cake, shrimp shells and green seaweed, and the protein isolates produced from herring co-products wo/w different helpers. SST = Single-stage toothed, RD = Radial discharge.

when cross-processing herring co-products with lingonberry press-cake and green seaweed. This could be related to the reduction of the aggregation of certain polysaccharides as reflected by the largely reduced consistency of homogenates. During the solubilization step, herring proteins may strongly interact with polysaccharides during their own swelling, resulting in co-precipitation during the first centrifugation step, whereupon the proteins end up in the sediment which is then removed (Dhouafli et al., 2018). In presence of green seaweed, the protein solubilization *per se* was not enhanced (Table 1), but the amount of supernatant which could be recovered after the first centrifugation increased from 81.7 ± 2.4 to 87.6 ± 0.4 ml per 100 ml of homogenate, pointing at reduced polysaccharide swelling as the main reason for higher solubilization yields. That US reduced the particle size of the seaweed could be visually observed. With shrimp shells, the use of US reduced solubilization yield and total protein yields, which was possibly because US promoted the release of $CaCO_3$ and other shrimp shell-constituents that induced precipitation of the proteins (Polowczyk et al., 2016).

3.2. Formation of lipid oxidation-derived aldehydes during processing

MDA and HHE were used to monitor lipid oxidation during processing. As shown in Table 2, significant increase of MDA and HHE contents was detected in the control protein isolates compared to the fresh herring co-products, indicating the occurrence of lipid oxidation during processing. This finding aligned with our previous studies (Abdollahi et al., 2020; Zhang et al., 2022) and reaffirmed the importance of limiting lipid oxidation during pH-shift processing. The change of homogenizer into RD-HSMH significantly increased carbonyl levels during processing, while US significantly decreased the levels. The pro-oxidative impacts of RD-HSMH could be explained by that RD-HSMH enhanced the disruption of highly organized fish muscle microstructure and removal of surrounding connective tissues compared with SST-HSMH, which lead to better exposure of the membranal phospholipids to Hb and other prooxidants, therefore promoting lipid oxidation (Marmon, Krona, Langton, & Undeland, 2012). US was earlier reported to increase the rate and extent of lipid oxidation measured as TBARS during the curing treatment of raw beef, and the content of TBARS increased with the increasing intensity (2.39–20.96 W/cm^2) of US (Kang et al., 2016). That carbonyl levels instead decreased in our study could be due to stimulation of reactions between carbonyls and the herring proteins or phospholipids, yielding e.g. Schiff's bases (Domingues, Domingues, Melo, Pérez-Sala, Reis, & Spickett, 2013). US could also disrupt the highly organized fish muscle microstructure and remove surrounding connective tissues, which can lead to better exposure of the membranal phospholipids to e.g. carbonyls (Marmon et al., 2012). In presence of helper raw materials, the formation of MDA and HHE was dependent on the type of helper and the specific treatments applied during cross-processing. In line with our earlier findings (Abdollahi et al., 2020; Zhang et al., 2022), lingonberry press-cake showed the best antioxidant capacity among the three helpers, reflected by the extremely low MDA and HHE levels detected in its corresponding protein isolates regardless of the treatment applied (Table 2). A significant antioxidant capacity of lingonberry press-cake when added directly to herring mince has also been reported by others (Damerau et al., 2020) and it is likely attributed to the abundance of e.g. proanthocyanidins, hydroxycinnamic acid derivatives (HCA), flavonols, and arbutin derivatives in leaves; as well as anthocyanins and benzoic acid (e.g. benzoyl glucose) in the fruits (Bujor, Ginies, Popa, & Dufour, 2018). With the addition of shrimp shells, SST-HSMH-produced protein isolates showed significantly lower MDA and HHE contents compared to the shrimp-free controls, which was in agreement with our previous study (Abdollahi et al., 2020). Applying RD-HSMH (-/+) US gave the same carbonyl levels which were higher than when using SST-HSMH. The lack of effect was in line with our recent study, where shrimp shells had no significant impacts on lipid oxidation in herring co-products during alkali-aided pH-shift processing comprising RD-HSMH (Zhang et al., 2022). The lack of antioxidant capacity was hypothesized to be related to poor extraction of astaxanthin during the process with RD-HSMH. Astaxanthin is a lipid-soluble antioxidant abundant in shrimp peeling co-products (Khumallambam, Rama, Karuppannan, & Manjabhat, 2011). Significant amounts of astaxanthin are bound to shrimp proteins (Khumallambam et al., 2011), and ~ 50 % of the total astaxanthin was earlier shown to be extracted to the protein isolates produced by the alkali-aided pH-shift method with SST-homogenizer using pH 10 and pH 4.5 for solubilization and precipitation, respectively (Khumallambam et al., 2011). In the present study, US was hypothesized to promote astaxanthin extraction during the solubilization step prior to the first centrifugation, counteracting astaxanthin losses into the non-soluble and discarded pellet. However, when comparing the protein isolates produced with shrimp shells without and with US, no significant differences were found neither in their protein contents (Table 2) nor in their polypeptide patterns (Fig. 2), implying that astaxanthin extraction was not enhanced and therefore it did not protect the herring protein

Table 2
Lipid oxidation-derived aldehyde contents and proximate composition of raw materials (herring co-products, lingonberry press-cake, shrimp shells, green seaweed) and protein isolates produced from herring co-products wo/w different helpers. Aldehyde data are given as μmol/kg on a wet weight basis (ww). Protein, lipid and ash data are given as g/100 g dry weight (dw). Data are shown as mean values ± standard deviation (n ≥ 2). SST = Single-stage toothed, RD = Radial discharge.

Type	Source	Treatment*	Lipid oxidation-derived aldehydes		Proximate composition		
			MDA	HHE	Protein	Lipid	Ash
Fish co-products	Herring co-products		8.3 ± 0.1^{f}	0.26 ± 0.02^{g}	48.7 ± 1.2^{f}	32.7 ± 1.5^{a}	14.5 ± 0.2^{c}
Helpers	Lingonberry press-cake		$<4^{f}$	$<0.04^{h}$	5.6 ± 0.1^{i}	14.4 ± 2.1^{gh}	2.0 ± 0.2^{j}
	Shrimp shells		$<4^{f}$	$<0.04^{h}$	39.8 ± 0.1^{g}	7.7 ± 0.5^{j}	62.4 ± 0.4^{a}
	Green seaweed		10.3 ± 0.4^{f}	0.29 ± 0.01^{g}	15.4 ± 0.1^{h}	7.0 ± 0.1^{j}	28.3 ± 0.1^{b}
Protein isolates	Herring co-products	SST-HSMH	176.8 ± 0.1^{b}	2.17 ± 0.12^{b}	82.1 ± 1.7^{a}	15.0 ± 0.5^{efg}	3.3 ± 0.2^{hi}
		RD-HSMH	206.1 ± 4.6^{a}	1.21 ± 0.05^{e}	79.9 ± 1.4^{ab}	14.0 ± 0.2^{gh}	3.2 ± 0.1^{hi}
		RD-HSMH+US	141.7 ± 7.9^{c}	3.19 ± 0.08^{a}	77.4 ± 0.5^{b}	17.5 ± 0.3^{c}	3.5 ± 0.1^{h}
	Herring co-products +Lingonberry press-cake	SST-HSMH	$<4^{f}$	$<0.04^{h}$	72.4 ± 0.2^{c}	14.0 ± 0.8^{gh}	4.2 ± 0.2^{g}
		RD-HSMH	$<4^{f}$	$<0.04^{h}$	74.5 ± 0.7^{c}	13.3 ± 1.6^{h}	3.0 ± 0.1^{hi}
		RD-HSMH+US	$<4^{f}$	$<0.04^{h}$	67.6 ± 0.0^{d}	16.6 ± 0.3^{cd}	6.2 ± 0.0^{e}
	Herring co-products +Shrimp shells	SST-HSMH	156.0 ± 5.8^{c}	1.56 ± 0.17^{d}	79.0 ± 0.7^{b}	17.3 ± 0.5^{c}	3.0 ± 0.0^{i}
		RD-HSMH	184.6 ± 2.2^{b}	1.82 ± 0.09^{c}	78.9 ± 0.4^{b}	15.7 ± 0.3^{def}	4.3 ± 0.2^{g}
		RD-HSMH+US	175.9 ± 1.5^{b}	1.78 ± 0.02^{c}	79.4 ± 0.4^{b}	20.7 ± 0.9^{b}	3.1 ± 0.0^{hi}
	Herring co-products +Green seaweed	SST-HSMH	143.7 ± 5.5^{c}	1.49 ± 0.01^{d}	61.7 ± 0.5^{e}	14.6 ± 0.4^{fg}	3.3 ± 0.0^{hi}
		RD-HSMH	124.0 ± 3.8^{d}	1.17 ± 0.00^{e}	72.7 ± 0.2^{c}	11.9 ± 0.0^{i}	4.8 ± 0.0^{f}
		RD-HSMH+US	106.4 ± 3.2^{e}	0.89 ± 0.01^{f}	72.4 ± 1.3^{c}	15.8 ± 0.2^{de}	8.3 ± 0.1^{d}

Different small letters in each column show a significant difference ($p < 0.05$).
*SST-HSMH and RD-HSMH imply raw materials were treated by a SST homogenizer at 10,000 rpm for 60 s, or by a RD homogenizer at 8,000 rpm for 90 s. RD-HSMH was more efficient than SST-HSMH in dispersing raw materials. US was applied to pH-adjusted homogenates during the protein solubilization step.

isolates towards oxidation. It may however be possible to optimize the US treatments for better extraction of astaxanthin in future studies. Green seaweed (*Ulva fenestrata*) significantly reduced the content of MDA and HHE measured in protein isolates compared to the controls, which was aligned with our previous study (Zhang et al., 2022). Promising antioxidant capacity of green seaweed extracts *in vitro* has also been reported by others using several assays; DPPH·, ABTS·+, hydroxyl and superoxide radical scavenging ability, as well as ferrous ion chelating ability (Peasura, Laohakunjit, Kerdchoechuen, & Wanlapa, 2015; Qi et al., 2005). SST-HSMH was earlier reported to assist protein and carbohydrate extraction from green seaweed (*Ulva lactuca*) by disintegrating the macrostructure of seaweed efficiently (Postma et al., 2017). As shown in Table 2, changing homogenizer significantly limited the formation of MDA and HHE in presence of *U. fenstrata*, which was further reduced by US. These findings could be explained by a better extraction of antioxidants from the seaweed by RD-HSHM and US. US has been reported to assist the extraction of antioxidants from green seaweed (*Ulva lactuca*) (Rashad, El-Chaghaby, Lima, Simoes, & Reis, 2021), as reflected by a promising total antioxidant capacity of the extracts determined by using the phosphomolybdenum method (Prieto, Pineda, & Aguilar, 1999).

3.3. Proximate composition of protein isolates

As shown in Table 2, the addition of the three helpers generally yielded a lower protein content in the cross-processed protein isolates compared to herring controls, which was in agreement with our earlier study (Abdollahi et al., 2020; Zhang et al., 2022). Applying RD-HSMH only showed significant impacts on the protein isolate produced with green seaweed – here the protein content increased from 61.7 to 72.7 g/100 g, dw, which could be explained e.g., by more selective extraction of seaweed proteins or the prevention of herring proteins losses. US rendered a reduced protein content ($p < 0.05$) of the protein isolates produced with lingonberry press-cake and showed no significant impacts on the protein isolates produced with green seaweed. These effects could be related to the superior effect of US in co-extracting also non-protein compounds, e.g., carbohydrates from lingonberry press-cake and green seaweed, therefore diluting protein in the final protein isolates.

The pH-shift processing of herring co-products wo/w helpers showed good lipid-removal ability reflected by the significantly ($p < 0.05$) lower lipid contents measured in protein isolates compared to herring co-products. This was in agreement with our earlier results (Abdollahi et al., 2020; Zhang et al., 2022). During protein solubilization, neutral storage lipids and membrane-bound phospholipids can be separated from the solubilized proteins based on their density and polarity (Kristinsson, Theodore, Demir, & Ingadottir, 2005) generating a floating fat layer and sediment, respectively, when the centrifugation force is high enough. The main differences in presence of helpers compared to without them were that shrimp shells rendered a higher lipid content with all processing modifications, which could be related to the unstable fat layer formed leading to inefficient lipid removal, as we also observed in our earlier study (Abdollahi et al., 2020; Zhang et al., 2022). Further, the addition of green seaweed together with RD-HSMH wo/w US significantly reduced lipid content which could be explained by the increased system polarity resulting from the increased co-extraction of phenolic compounds (Rodrigues et al., 2015) and salts. US resulted in significantly ($p < 0.05$) higher lipid content in all protein isolates most likely since it is more effective for dispersing material as it enables higher curvature of fat droplets, thereby creating very weak floating fat layers for all raw materials, which were hard to remove.

High ash content was measured in the herring co-products as well as in shrimp shells and green seaweed helpers, but it was dramatically decreased ($p < 0.05$) during pH-shift processing (Table 1) reflecting its efficiency in sedimenting insoluble impurities such as fish bones, shells and connective tissue during centrifugation. Replacing SST-HSMH by RD-HSMH yielded higher ash content in protein isolates produced with shrimp shells and green seaweed, possibly due to the efficiency of RD-HSMH to release more minerals from these helpers to the soluble fraction. On the other hand, the change of homogenizer significantly ($p < 0.05$) reduced the ash content with the presence of lingonberry press-cake. US dramatically increased ash contents of protein isolates produced with lingonberry press-cake or green seaweed, also explained by a promoted solubilization of minerals (Rodrigues et al., 2015).

3.4. Active sulfhydryl groups and total sulfhydryl groups

Sulfhydryl groups play important roles in protein functionalities. As shown in Table 3, the amount of total and active sulfhydryl groups in protein isolates depended on both the combination of raw materials and the treatment applied during cross-processing. The addition of helpers generally rendered a higher content of active and total sulfhydryl groups in the final protein isolates. The highest amount of total and active sulfhydryl groups was found in the protein isolates produced with green seaweed treated by RD-HSMH. Except for in the combination with lingonberry press-cake, replacing SST-HSHM by RD-HSMH generally yielded higher contents of total and active sulfhydryl groups, as well as a lower ratio of active to total sulfhydryl groups which could be due to protein unfolding, exposing internal sulfhydryl groups (Yin et al., 2019). In presence of lingonberry press-cake, replacing SST-HSHM by RD-HSMH increased this ratio from 63 % to 76 %. The higher ratio of active to total sulfhydryl groups indicates a better exposure of the sulfhydryl groups to the solvent, which may imply a higher degree of conformational changes occurred during the pH-shift-based cross-processing (Villamonte, Pottier, & de Lamballerie, 2015). US generally increased the content of active and total sulfhydryl groups of the proteins recovered from herring co-products +/− lingonberry press-cake but caused a reduction for the protein isolates produced with shrimp shells and green seaweed. The increased contents could be explained by the breakage of intermolecular disulfide bonds and exposure of the buried sulfhydryl groups due to the cavitation phenomenon (Li et al., 2020). On the other hand, the decreased contents could be due to the oxidation of susceptible sulfhydryl groups induced by cavitation-generated hydrogen peroxide, and/or a partial aggregation of proteins caused by the high US power and re-encapsulation of some sulfhydryl groups (Hu et al., 2013).

3.5. Surface hydrophobicity

As presented in Table 3, regardless of the type of helper, cross-processing by itself significantly increased the surface hydrophobicity of herring proteins, which implies that helpers stimulated molecular unfolding, exposing originally buried hydrophobic groups (Li et al., 2020), or that proteins or peptides with higher surface hydrophobicity were co-extracted from the helpers. Replacing SST-HSHM by RD-HSMH significantly decreased the surface hydrophobicity of proteins recovered with lingonberry press-cake or with green seaweed. US improved surface hydrophobicity from 68.1 to 82.1 for protein isolates produced with lingonberry press-cake, which indicated protein conformational changes induced by the cavitation and shear stress generated by US treatment. In addition, US may induce hydrophobic interactions by rendering minor conformational changes, decreasing protein hydrophobicity (Malik, Sharma, & Saini, 2017). Similarly, Sun et al. (2014) found that harsh US treatment with high US power and time, led to a decrease in the protein surface hydrophobicity due to aggregation and re-polymerization of milk proteins.

3.6. Polypeptide pattern

The electrophoretic patterns of protein isolates under reducing conditions are presented in Fig. 2. As can be seen, herring co-products and all protein isolates were abundant e.g. in myosin heavy chain (MHC) (~205 kDa), myosin light chain (~25 kDa) as well as actin (~42 kDa), and were very similar to the polypeptide pattern earlier reported for gutted herring proteins (Marmon & Undeland, 2010). This reveals that cross-processing did not have a big impact on the overall

Table 3
Sulfhydryl groups and surface hydrophobicity, water solubility, emulsion activity index (EAI) and emulsion stability index (ESI) of protein isolates produced from herring co-products wo/w lingonberry press-cake (LPC), shrimp shells (SS) or green seaweed (GS). Data are given as mean values ± standard deviation (n = 3). SST = Single-stage toothed, RD = Radial discharge.

Source	Treatment*	Sulfhydryl groups			Hydrophobicity	Water solubility		EAI		ESI	
		Active SH (μmol/g)	Total SH (μmol/g)	Active to total (%)		At pH 7 (%)	At pH 11 (%)	At pH 7 (m^2/mg)	At pH 11 (m^2/mg)	At pH 7 (min)	At pH 11 (min)
Herring	SST-HSMH	11.5 ± 0.1^{h}	15.9 ± 0.2^{i}	72.2	46.1 ± 4.2^{h}	7.7 ± 0.4^{c}	36.9 ± 1.3^{g}	22.1 ± 0.2^{e}	53.2 ± 1.9^{f}	4.6 ± 0.0^{cd}	101.4 ± 8.1^{fg}
	RD-HSMH	13.6 ± 0.1^{g}	22.5 ± 0.4^{h}	60.4	42.9 ± 5.0^{h}	7.4 ± 0.8^{c}	41.5 ± 4.6^{fg}	20.8 ± 1.6^{f}	53.5 ± 1.3^{f}	8.1 ± 1.0^{b}	211.4 ± 0.5^{ef}
	RD-HSMH+US	15.0 ± 0.1^{f}	23.7 ± 0.3^{gh}	63.3	46.6 ± 2.7^{h}	6.8 ± 0.2^{c}	45.8 ± 2.1^{f}	13.1 ± 0.3^{h}	66.4 ± 2.1^{e}	5.8 ± 0.2^{c}	64.8 ± 0.4^{fg}
+LPC	SST-HSMH	16.6 ± 0.3^{e}	26.2 ± 0.0^{fg}	63.4	106.1 ± 5.3^{a}	12.6 ± 0.3^{a}	88.6 ± 0.8^{b}	32.6 ± 0.8^{a}	87.8 ± 5.5^{d}	9.8 ± 0.4^{b}	18.0 ± 2.2^{g}
	RD-HSMH	13.9 ± 0.3^{g}	18.3 ± 0.4^{i}	76.1	68.1 ± 6.3^{g}	9.7 ± 0.1^{b}	79.6 ± 0.5^{c}	28.3 ± 0.9^{bc}	93.5 ± 2.4^{c}	19.5 ± 1.3^{a}	1012.1 ± 13.0^{c}
	RD-HSMH+US	17.0 ± 0.4^{e}	25.9 ± 0.8^{fg}	65.7	82.1 ± 2.8^{de}	9.3 ± 0.8^{b}	70.9 ± 1.0^{d}	22.7 ± 0.9^{e}	68.8 ± 0.4^{e}	9.0 ± 1.4^{b}	10.8 ± 1.3^{g}
+SS	SST-HSMH	21.5 ± 0.0^{b}	31.2 ± 1.7^{cd}	68.9	98.4 ± 1.0^{ab}	10.4 ± 0.4^{b}	94.7 ± 1.7^{a}	19.1 ± 0.1^{g}	87.1 ± 0.9^{d}	3.1 ± 0.0^{d}	497.3 ± 3.3^{d}
	RD-HSMH	21.0 ± 0.3^{bc}	36.1 ± 0.7^{b}	58.1	97.0 ± 1.8^{abc}	10.4 ± 0.2^{b}	74.7 ± 0.9^{cd}	21.9 ± 0.3^{e}	34.2 ± 0.2^{g}	9.4 ± 1.1^{b}	120.5 ± 7.1^{fg}
	RD-HSMH+US	13.4 ± 0.0^{g}	28.1 ± 0.2^{ef}	47.8	86.2 ± 3.1^{cde}	9.1 ± 0.3^{b}	58.6 ± 2.0^{e}	20.7 ± 0.2^{f}	99.0 ± 0.4^{ab}	5.5 ± 0.0^{c}	1201.7 ± 26.4^{b}
+GS	SST-HSMH	20.2 ± 0.1^{c}	29.0 ± 0.2^{de}	69.7	86.2 ± 3.1^{cde}	12.2 ± 0.0^{a}	80.5 ± 1.4^{c}	27.5 ± 0.6^{cd}	97.3 ± 1.8^{bc}	2.5 ± 0.3^{d}	74.5 ± 19.3^{fg}
	RD-HSMH	27.8 ± 0.4^{a}	42.1 ± 1.2^{a}	66.1	79.7 ± 3.3^{ef}	13.0 ± 0.5^{a}	64.0 ± 1.8^{e}	29.0 ± 0.2^{b}	102.2 ± 0.6^{a}	3.5 ± 0.1^{cd}	3944.0 ± 154.6^{a}
	RD-HSMH+US	18.4 ± 0.3^{d}	32.6 ± 1.7^{c}	56.6	68.9 ± 0.6^{fg}	10.0 ± 0.1^{b}	36.6 ± 0.1^{g}	27.3 ± 0.1^{d}	57.2 ± 6.3^{f}	3.0 ± 0.0^{d}	326.7 ± 16.2^{e}

Different small letters in each column show a significant difference ($p < 0.05$).
*SST-HSMH and RD-HSMH imply raw materials were treated by a SST homogenizer at 10,000 rpm for 60 s, or by a RD homogenizer at 8,000 rpm for 90 s. RD-HSMH was more efficient than SST-HSMH in dispersing raw materials. US was applied to pH-adjusted homogenates during the protein solubilization step.

polypeptide composition of herring proteins. Compared to the polypeptide pattern of herring co-products, protein isolates derived thereof with classic pH-shift processing presented a few bands below MHC, suggesting slight proteolysis. This was also seen with green seaweed but was counteracted by lingonberry press-cake, which also darkened the area above MHC illustrating possible protein crosslinking. For herring protein isolates produced without and with the helpers, the change of homogenizer to RD-HSMH yielded a more intensive MHC band, which was reduced by US. The use of US for herring co-products alone revealed slight MHC degradation, most likely caused by acoustic cavitation and streaming which led to violent shear force between solvent and protein molecules (Tian et al., 2015), or by activation of endogenous protease(s) (Soria & Villamiel, 2010). However, this effect was not seen when applying US during cross-processing with the three helpers.

3.7. Water solubility of protein isolates

The solubility in water is an important characteristic of proteins that influences many other protein functionalities such as emulsifying, foaming and gelation properties, and was here measured at pH 7 and pH 11 (Table 3). Solubility at pH 7 was much lower than at pH 11 for all samples, which aligned with the nature of non-processed herring proteins (Fig. 1). Herring protein isolates produced without helpers had 6–8 % solubility at pH 7 and 36–46 % at pH 11, which was in a similar range as reported earlier (Abdollahi & Undeland, 2018). Neither the change of homogenizer nor the use of US significantly affected protein solubility at pH 7; while at pH 11, the protein solubility significantly increased by replacing SST-HSMH by RD-HSMH plus using US. This could be related to the cavitation effect of US disrupting Van de Waals forces, hydrogen bonding and dipole attractions between the molecules and promoting their water solubility (Li et al., 2020).

When introducing helpers, the solubility of protein isolates significantly ($p < 0.05$) increased for most samples at pH 7 and pH 11; up to 2–3-fold compared to herring controls. The helpers probably influenced the unfolding and refolding pattern of proteins during the pH-shift processing leading to a higher exposure of polar groups (Li et al., 2020). The protein isolates produced with lingonberry press-cake were most affected by the change of homogenizer: RD-HSHM rendered significantly lower solubility at both pH 7 and pH 11. For the combinations with shrimp shells or green seaweed, RD-HSMH significantly decreased solubility at pH 11, which was further decreased by US. Aligned with the decreased ratio of active SH to total SH groups as well as surface hydrophobicity of the protein isolates caused by RD-HSMH + US (Table 3), this could be due to protein aggregation. Overall, this study revealed a positive correlation between, on the one hand, increased sulfhydryl content and protein surface hydrophobicity and on the other increased solubility, which was in agreement with the studies of Lee et al. (2016); and Wagner et al. (2000), respectively.

3.8. Emulsifying properties of protein isolates

Emulsion activity index (EAI) and emulsion stability index (ESI) of all protein isolates at pH 3, 5, 7, 9 and 11 were determined, with results obtained at pH 7 and pH 11 presented in Table 3, and complete data in **supplementary** table 2-3. EAI of proteins reflects their capacity to cover the oil/water interface. As shown in **Table 4**, the EAI of all protein isolates was lower at pH 7 than 11, correlating to their water solubility (Table 3). It was thus clear that moving away from the pI (~pH 5), which increases the net charge of the protein molecules, weakened the interactions and thereby enhancing their emulsifying properties (Chen, Zhou, Xu, Zhou, & Liu, 2017). Cross-processing itself, regardless of the type of helper, generally increased the protein EAI at pH 7 and pH 11, which also agreed with the ability of helpers to increase water solubility (Table 3) and surface hydrophobicity (Table 3); the latter reducing the energy barrier at the oil–water interface, thus increasing the adsorption kinetics. Other components co-extracted from the helpers during the

cross-processing, e.g., phospholipids, could also play important roles for the raised EAI. The effects of changing homogenizer and applying US were dependent on the type of helpers. At pH 7, the highest and lowest EAIs were measured for protein isolates produced with lingonberry press-cake and shrimp shells, respectively by SST-HSMH (32.6 m^2/mg *vs* 19.1 m^2/mg). At pH 11, the highest and lowest EAIs were found after the addition of green seaweed and shrimp shells, respectively, using RD-HSMH (102.2 m^2/mg *vs* 34.2 m^2/mg).

As shown in Table 3, ESI at pH 7 was in the range of 2–20 min, which was significantly lower than at pH 11 (65–4000 min). Three samples presented significantly higher ESI at pH 11 compared to the other nine, which were the protein isolates produced using RD-HSMH with lingonberry press-cake (1012 min), with shrimp shells plus US (1202 min) and with green seaweed (3944 min). US generally lowered ESI, which could be related to the lower molecular weight (LMW) polypeptides/peptides generated. It has been reported that higher content of high molecular weight (HMW) peptides stabilizes an emulsion (Schröder, Berton-Carabin, Venema, & Cornacchia, 2017) while LMW peptides and amino acids are less efficient in reducing the interfacial tension due to lack of unfolding and reorientation at the interface (Klompong, Benjakul, Kantachote, & Shahidi, 2007). The more intense MHC band found in isolates made with helpers (Fig. 2) may hereby explain the higher emulsifying properties of the cross-processed protein isolates.

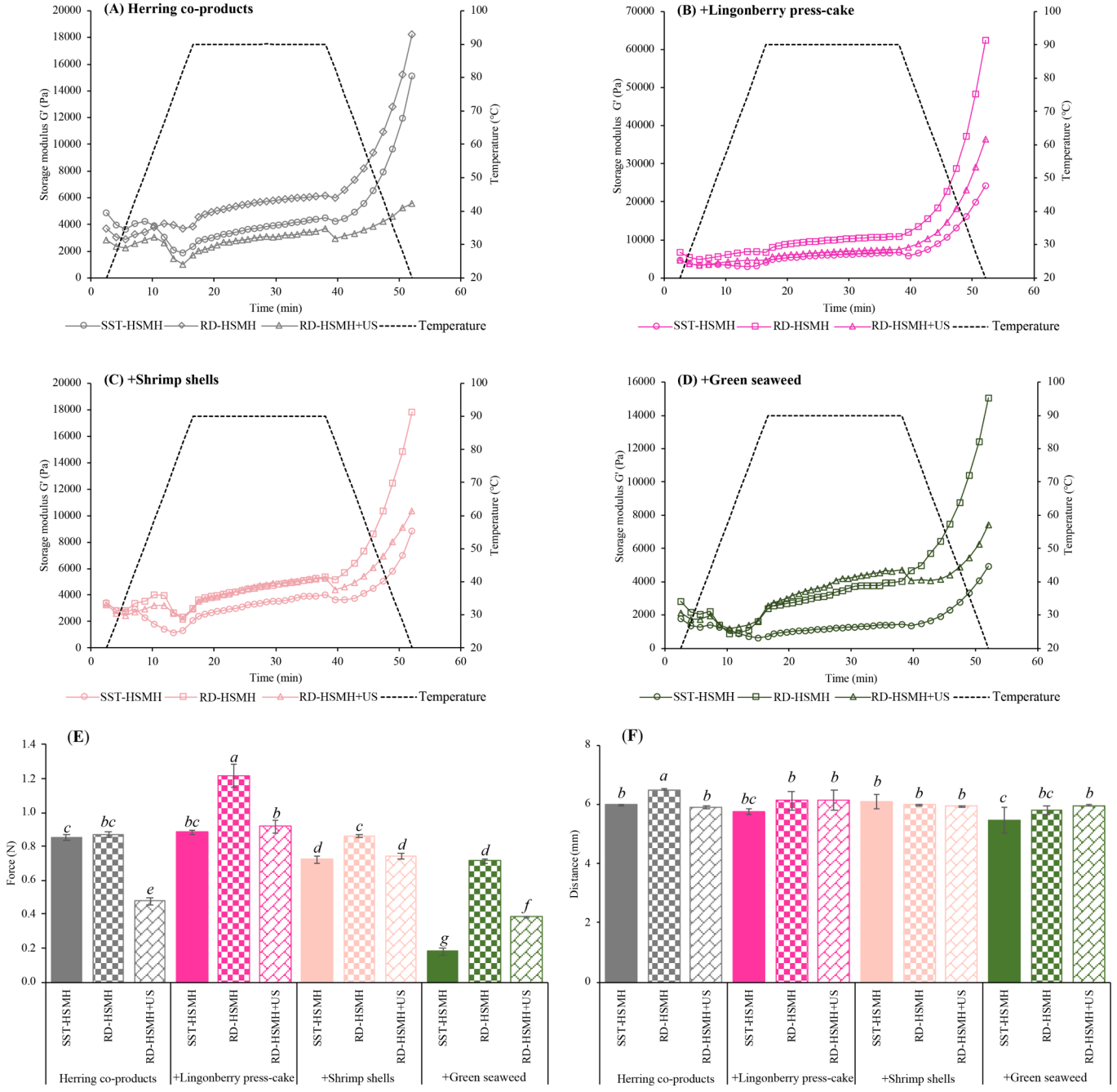

Fig. 3. Temperature ramp tests performed for protein isolates (moisture = 80 %, pH = 7) produced from herring co-product alone (A) or its combination with lingonberry press-cake (B), shrimp shells (C) and green seaweed (D). An initial heating step (rate: 1 °C/min from 20 to 90 °C) was followed by an isothermal step (90 °C, 30 min) and a final cooling step (rate: 1 °C/min from 90 to 20 °C). Breaking force (E) of the produced gels, and the distance that the probe entered the gel (F) measured by puncture test. Different small letters in each column show a significant difference ($p < 0.05$). SST = Single-stage toothed, RD = Radial discharge.

3.9. Evolution of storage moduli of protein isolates during gelation and puncture test of the produced gels

As shown in Fig. 3 **A-D**, the evolution of storage modulus (G') over the thermal cycle was different between different protein isolates, but the gelation profile was similar to other typical protein gelation processes (Dapčević-Hadnađev, Hadnađev, Lazaridou, Moschakis, & Biliaderis, 2018; Felix et al., 2017a, 2017b). During the early heat-up process up to 40 °C, the reduction of G' observed for all samples could be attributed to an increase in mobility of the protein chains induced by thermal agitation, reducing physical interactions due to fracture of electrostatic and hydrogen bonds (Felix, Romero, Rustad, & Guerrero, 2017b). During the further heat-up process to 90 °C, the increase of G' can be attributed to the formation of a three-dimensional network via partially denatured proteins either in the form of globular proteins or of helical rod segments of myosin which promote network formation through sulfide-bonds (Felix et al., 2017b; Romero, Bengoechea, Cordobés, & Guerrero, 2009; Westphalen, Briggs, & Lonergan, 2006). Samples with different helpers and treated with different assistant technologies showed differences in their G' evolution in this step of the gelation which could reflect differences in their structure formation via chemical bonds and especially disulfide bonds. During the isothermal treatment at 90 °C, G' rose slowly for all samples, indicating that the formation of disulfide-bonds of the helical rod segments of myosin was stronger than the electrostatic repulsion between protein chains, reflecting weak protein surface charges (Felix, Romero, Rustad, & Guerrero, 2017a). Finally, when performing the cooling step, a steady increase in G' was observed for all samples, although some of them presented a smooth decline in the beginning, implying structure reinforcement due to the reformation of e.g. hydrogen and hydrophobic bonds (Felix et al., 2017a). This could also imply that the gels produced were mostly stabilized with hydrogen and hydrophobic bonds formed during the cooling step where the highest evolution in the G' for all the samples when they reached their maximum G' at 20 °C at the end. For the herring control samples, the change of homogenizer improved G' at this stage from 15 kPa to 18 kPa, while US reduced it to a value being the second-lowest among the twelve samples (5.6 kPa). For the cross-processed protein isolates, RD-HSMH generally rendered the highest G' among the three processing versions, while US reduced G'. The effect of RD-HSMH could be related to the higher protein contents and lower lipid contents of protein isolate produced with this homogenization (Table 2), while opposite, the effect of US may be attributed to the significantly increased lipid contents of US-produced protein isolates (Table 2) (Chaijan, Panpipat, & Benjakul, 2010), as well as the protein aggregations and degradations caused by US. In the case of the control sample, the high degradation of myosin heavy chain observed in the SDS-PAGE results could partly explain the poor structure formation of the US treated samples. In addition, almost all US treated samples showed poorer structure formation capacity during the cooling step which could show their lower ability to form hydrogen bonds and hydrophobic interactions which are necessary for the final stabilization of the protein three-dimensional structure in the gels. Compared to the others, protein isolates made with lingonberry press-cake presented higher G' during the heat-up, holding at 90℃ and cooling step, this was especially true for the protein isolates produced by using RD-HSMH, which had by far the highest end G' (62 kPa). The lowest G' among the twelve samples was provided by the protein isolate produced with SST-HSMH and green seaweed, most likely due to its low protein content (Table 2).

Fig. 3 **E-F** demonstrates the breaking force of the produced gels and the distance that the probe entered the gel, the former agreeing well with the G' results (Fig. 3 **A-D**). As can be seen in Fig. 3 **E-F**, adding helpers significantly impacted both breaking force and distance in most cases, but the effect depended on the type of helper and processing methods. Lingonberry press-cake significantly increased the breaking force when using RD-HSMH wo/w US, the former one presenting the highest breaking force among the twelve samples. On the other hand, green seaweed significantly reduced the breaking force, and the one produced by SST-HSMH showed the lowest breaking force among all samples, possibly attributed to that it had the lowest protein content (Table 2). When comparing the different treatments, RD-HSMH generally rendered the highest breaking force which could be related to the lower lipid content (Table 2) (Chaijan et al., 2010) of isolates from this treatment. Interestingly, the application of RD-HSMH could, to a large extent, compensate the negative effect of cross-processing with shrimp and seaweed on the puncture force. In contrast, US decreased breaking force, most likely related to the fact that it induced protein aggregations, degradations of myosin (Fig. 2) and increased lipid contents (Table 2).

4. Conclusions

This study confirmed our earlier findings that combining fish co-products with antioxidant-rich raw materials during pH-shift processing ("cross-processing") prevented lipid oxidation, but at the same time hampered protein solubility and solubilization yields. When adding shrimp shells or green seaweed, the reductions in solubilization yield were larger for acid- than alkaline solubilization, therefore shrimp shells or green seaweed can only be recommended as helpers when using alkaline solubilization. An increased amount of water counteracted protein yield losses for all combinations of raw materials, and for shrimp shells or green seaweed, replacing SST- by RD-HSMH also showed positive effects. US further increased protein yields for the combinations with lingonberry press-cake or green seaweed; the latter approaching the protein yield obtained for herring co-products alone with classic pH-shift processing. Cross-processing itself largely increased the stability towards lipid oxidation, water solubility and emulsification activity of produced protein isolates; particularly with lingonberry press-cake which also improved gel-forming capacity. Changing from SST- to RD-HSMH generally improved lipid oxidative stability, as well as protein emulsifying and gelation properties of the produced protein isolates but reduced their protein water solubility. In general, the RD-homogenizer was a more suitable option during cross-processing. US improved the lipid oxidative stability of the produced protein isolates with green seaweed, but overall it negatively affected the structural and functional properties of the protein isolates and would thus need further studies to take advantage of its positive effect on yield.

Altogether, when cross-processing herring co-products with lingonberry press-cake, shrimp shells or green seaweed, it was recommended to use a raw material to water ratio of 1:6, and RD-driven homogenization at 8000 rpm for 90 s, without using US. The solubilization pH was optimized to pH 12 for all combinations of raw materials while the precipitation pH had to be tailored to the helper with pH 5 being optimal for lingonberry press-cake and shrimp shells while pH 4.5 was most suitable for green seaweed. In addition, the results showed that the positive effect of cross-processing is not limited to minimizing lipid oxidation but also improves protein functionality if using the right processing conditions. Cross-processing herring co-products with lingonberry press-cake using RD-HSMH was particularly promising and deserves further studies e.g., of sensorial and nutritional properties.

CRediT authorship contribution statement

Jingnan Zhang: Conceptualization, Methodology, Investigation, Formal analysis, Writing – original draft, Visualization. **Anna Ström:** Writing – review & editing. **Romain Bordes:** Writing – review & editing. **Marie Alminger:** Resources, Writing – review & editing. **Ingrid Undeland:** Conceptualization, Funding acquisition, Writing – review & editing. **Mehdi Abdollahi:** Conceptualization, Methodology, Writing – review & editing.

Declaration of Competing Interest

The authors declare that they have no known competing financial interests or personal relationships that could have appeared to influence the work reported in this paper.

Data availability

Data will be made available on request.

Acknowledgments

The authors are grateful to Formas, the Swedish Research Council, for financial support of the research (project# 2016-00246). Also, the authors would like to thank *Sweden Pelagic AB*, *Grangärde Musteri AB, Räkor och Laxgrossisten AB* and *Sven Lovén Centre for Marine Infrastructure* for kindly providing herring filleting co-products, lingonberry press-cake, shrimp shells and green seaweed.

Appendix A. Supplementary data

Supplementary data to this article can be found online at https://doi.org/10.1016/j.foodchem.2022.133986.

References

Abdollahi, M., Olofsson, E., Zhang, J., Alminger, M., & Undeland, I. (2020). Minimizing lipid oxidation during pH-shift processing of fish by-products by cross-processing with lingonberry press cake, shrimp shells or brown seaweed. *Food Chemistry, 327*, Article 127078. https://doi.org/10.1016/j.foodchem.2020.127078

Abdollahi, M., Rezaei, M., Jafarpour, A., & Undeland, I. (2019). Effect of microbial transglutaminase and setting condition on gel properties of blend fish protein isolate recovered by alkaline solubilisation/isoelectric precipitation. *International Journal of Food Science and Technology, 54*(3), 762–770. https://doi.org/10.1111/ijfs.13991

Abdollahi, M., & Undeland, I. (2018). Structural, functional, and sensorial properties of protein isolate produced from salmon, cod, and herring by-products. *Food and Bioprocess Technology, 11*(9), 1733–1749. https://doi.org/10.1007/s11947-018-2138-x

Alvarez, C., Elu, P. L., Lynch, S. A., Tiwari, B. K., Álvarez, C., Lélu, P., … Tiwari, B. K. (2018). Optimised protein recovery from mackerel whole fish by using sequential acid/alkaline isoelectric solubilization precipitation (ISP) extraction assisted by ultrasound. *LWT - Food Science and Technology, 88*, 210–216. https://doi.org/10.1016/j.lwt.2017.09.045

Bujor, O. C., Ginies, C., Popa, V. I., & Dufour, C. (2018). Phenolic compounds and antioxidant activity of lingonberry (Vaccinium vitis-idaea L.) leaf, stem and fruit at different harvest periods. *Food Chemistry, 252*, 356–365. https://doi.org/10.1016/j.foodchem.2018.01.052

Chaijan, M., Panpipat, W., & Benjakul, S. (2010). Physicochemical and gelling properties of short-bodied mackerel (Rastrelliger brachysoma) protein isolate prepared using alkaline-aided process. *Food and Bioproducts Processing, 88*(2–3), 174–180. https://doi.org/10.1016/j.fbp.2009.11.003

Chen, X., Zhou, R., Xu, X., Zhou, G., & Liu, D. (2017). Structural modification by high-pressure homogenization for improved functional properties of freeze-dried myofibrillar proteins powder. *Food Research International, 100*, 193–200. https://doi.org/10.1016/j.foodres.2017.07.007

Chomnawang, C., & Yongsawatdigul, J. (2013). Protein recovery of tilapia frame by-products by pH-shift method. *Journal of Aquatic Food Product Technology, 22*(2), 112–120. https://doi.org/10.1080/10498850.2011.629077

Czubinski, J., & Dwiecki, K. (2017). A review of methods used for investigation of protein-phenolic compound interactions. *International Journal of Food Science & Technology, 52*(3), 573–585. https://doi.org/10.1111/ijfs.13339

Damerau, A., Kakko, T., Tian, Y., Tuomasjukka, S., Sandell, M., Hopia, A., & Yang, B. (2020). Effect of supercritical CO2 plant extract and berry press cakes on stability and consumer acceptance of frozen Baltic herring (Clupea harengus membras) mince. *Food Chemistry, 332*, Article 127385. https://doi.org/10.1016/j.foodchem.2020.127385

Dapčević-Hadnađev, T., Hadnađev, M., Lazaridou, A., Moschakis, T., & Biliaderis, C. G. (2018). Hempseed meal protein isolates prepared by different isolation techniques. Part II. gelation properties at different ionic strengths. *Food Hydrocolloids, 81*, 481–489. https://doi.org/10.1016/j.foodhyd.2018.03.022

Das, A. B., Goud, V. V., & Das, C. (2017). Extraction of phenolic compounds and anthocyanin from black and purple rice bran (Oryza sativa L.) using ultrasound: A comparative analysis and phytochemical profiling. *Industrial Crops and Products, 95*, 332–341. https://doi.org/10.1016/j.indcrop.2016.10.041

Dhouafli, Z., Cuanalo-Contreras, K., Hayouni, E. A., Mays, C. E., Soto, C., & Moreno-Gonzalez, I. (2018). Inhibition of protein misfolding and aggregation by natural phenolic compounds. Issue 19. In *Cellular and Molecular Life Sciences* (pp. 3521–3538). Birkhauser Verlag AG. https://doi.org/10.1007/s00018-018-2872-2.

Domingues, R. M., Domingues, P., Melo, T., Pérez-Sala, D., Reis, A., & Spickett, C. M. (2013). Lipoxidation adducts with peptides and proteins: Deleterious modifications or signaling mechanisms? In *Journal of Proteomics* (Vol. 92, pp. 110–131). J Proteomics. doi:10.1016/j.jprot.2013.06.004.

FAO. (2020). The State of World Fisheries and Aquaculture 2020. In *The State of World Fisheries and Aquaculture 2020*. FAO. doi:10.4060/ca9229en.

Felix, M., Romero, A., Rustad, T., & Guerrero, A. (2017a). Physicochemical, microstructure and bioactive characterization of gels made from crayfish protein. *Food Hydrocolloids, 63*, 429–436. https://doi.org/10.1016/J.FOODHYD.2016.09.025

Felix, M., Romero, A., Rustad, T., & Guerrero, A. (2017b). Rheological properties and antioxidant activity of protein gels-like systems made from crayfish concentrate and hydrolysates. *Food and Bioproducts Processing, 102*, 167–176. https://doi.org/10.1016/J.FBP.2016.12.014

Geirsdottir, M., Hlynsdottir, H., Thorkelsson, G., & Sigurgisladottir, S. (2007). Solubility and viscosity of herring (Clupea harengus) proteins as affected by freezing and frozen storage. *Journal of Food Science, 72*(7). https://doi.org/10.1111/j.1750-3841.2007.00471.x

Gong, K. J., Shi, A. M., Liu, H. Z., Liu, L., Hu, H., Adhikari, B., & Wang, Q. (2015). Emulsifying properties and structure changes of spray and freeze-dried peanut protein isolate. *Journal of Food Engineering, 170*, 33–40. https://doi.org/10.1016/j.jfoodeng.2015.09.011

Hinchcliffe, J., Carlsson, N. G., Jönsson, E., Sundell, K., & Undeland, I. (2019). Aquafeed ingredient production from herring (Clupea harengus) by-products using pH-shift processing: Effect from by-product combinations, protein solubilization-pH and centrifugation force. *Animal Feed Science and Technology, 247*, 273–284. https://doi.org/10.1016/j.anifeedsci.2018.07.014

Hu, H., Wu, J., Li-Chan, E. C. Y., Zhu, L., Zhang, F., Xu, X., … Pan, S. (2013). Effects of ultrasound on structural and physical properties of soy protein isolate (SPI) dispersions. *Food Hydrocolloids, 30*(2), 647–655. https://doi.org/10.1016/J.FOODHYD.2012.08.001

Kang, D. C., Zou, Y. H., Cheng, Y. P., Xing, L. J., Zhou, G. H., & Zhang, W. G. (2016). Effects of power ultrasound on oxidation and structure of beef proteins during curing processing. *Ultrasonics Sonochemistry, 33*, 47–53. https://doi.org/10.1016/J.ULTSONCH.2016.04.024

Khumallambam, M., Rama, S., Karuppannan, R. R., & Manjabhat, S. N. (2011). Antioxidant activity of protein isolate obtained by the pH shift technique from hydrolyzed and unhydrolyzed shrimp processing discards. *Journal of Aquatic Food Product Technology, 20*(2), 209–221. https://doi.org/10.1080/10498850.2011.559618

Klompong, V., Benjakul, S., Kantachote, D., & Shahidi, F. (2007). Antioxidative activity and functional properties of protein hydrolysate of yellow stripe trevally (Selaroides leptolepis) as influenced by the degree of hydrolysis and enzyme type. *Food Chemistry, 102*(4), 1317–1327. https://doi.org/10.1016/j.foodchem.2006.07.016

Kristinsson, H. G., & Liang, Y. (2006). Effect of pH-shift processing and surimi processing on atlantic croaker (micropogonias undulates) muscle proteins. *Journal of Food Science, 71*(5). https://doi.org/10.1111/j.1750-3841.2006.00046.x

Kristinsson, H. G., Theodore, A. E., Demir, N., & Ingadottir, B. (2005). A comparative study between acid- and alkali-aided processing and surimi processing for the recovery of proteins from channel catfish muscle. *Journal of Food Science, 70*(4), C298–C306. https://doi.org/10.1111/j.1365-2621.2005.tb07177.x

Larsen, R., Eilertsen, K.-E., & Elvevoll, E. O. (2011). Health benefits of marine foods and ingredients. *Biotechnology Advances, 29*(5), 508–518. https://doi.org/10.1016/J.BIOTECHADV.2011.05.017

Lee, H., Yildiz, G., dos Santos, L. C., Jiang, S., Andrade, J. E., Engeseth, N. J., & Feng, H. (2016). Soy protein nano-aggregates with improved functional properties prepared by sequential pH treatment and ultrasonication. *Food Hydrocolloids, 55*, 200–209. https://doi.org/10.1016/j.foodhyd.2015.11.022

Li, Y., Cheng, Y., Zhang, Z., Wang, Y., Mintah, B. K., Dabbour, M., … Ma, H. (2020). Modification of rapeseed protein by ultrasound-assisted pH shift treatment: Ultrasonic mode and frequency screening, changes in protein solubility and structural characteristics. *Ultrasonics Sonochemistry, 69*, Article 105240. https://doi.org/10.1016/j.ultsonch.2020.105240

Malik, M. A., Sharma, H. K., & Saini, C. S. (2017). High intensity ultrasound treatment of protein isolate extracted from dephenolized sunflower meal: Effect on physicochemical and functional properties. *Ultrasonics Sonochemistry, 39*, 511–519. https://doi.org/10.1016/j.ultsonch.2017.05.026

Marcó, A., Rubio, R., Compañó, R., & Casals, I. (2002). Comparison of the Kjeldahl method and a combustion method for total nitrogen determination in animal feed. *Talanta, 57*(5), 1019–1026. https://doi.org/10.1016/S0039-9140(02)00136-4

Markwell, M. A. K., Haas, S. M., Bieber, L. L., & Tolbert, N. E. (1978). A modification of the Lowry procedure to simplify protein determination in membrane and lipoprotein samples. *Analytical Biochemistry, 87*(1), 206–210. https://doi.org/10.1016/0003-2697(78)90586-9

Marmon, S. K., Krona, A., Langton, M., & Undeland, I. (2012). Changes in salt solubility and microstructure of proteins from herring (clupea harengus) after pH-shift processing. *Journal of Agricultural and Food Chemistry, 60*(32), 7965–7972. https://doi.org/10.1021/jf301352s

Marmon, S. K., & Undeland, I. (2010). Protein isolation from gutted herring (Clupea harengus) using pH-shift processes. *Journal of Agricultural and Food Chemistry, 58*(19), 10480–10486. https://doi.org/10.1021/jf101057q

Ogunwolu, S. O., Henshaw, F. O., Mock, H. P., Santros, A., & Awonorin, S. O. (2009). Functional properties of protein concentrates and isolates produced from cashew (Anacardium occidentale L.) nut. *Food Chemistry, 115*(3), 852–858. https://doi.org/10.1016/j.foodchem.2009.01.011

Pearce, K. N., & Kinsella, J. E. (1978). Emulsifying Properties of Proteins: Evaluation of a Turbidimetric Technique. *Journal of Agricultural and Food Chemistry, 26*(3), 716–723. https://doi.org/10.1021/JF60217A041/ASSET/JF60217A041.FP.PNG_V03

Peasura, N., Laohakunjit, N., Kerdchoechuen, O., & Wanlapa, S. (2015). Characteristics and antioxidant of Ulva intestinalis sulphated polysaccharides extracted with different solvents. *International Journal of Biological Macromolecules, 81*, 912–919. https://doi.org/10.1016/j.ijbiomac.2015.09.030

Polowczyk, I., Bastrzyk, A., & Fiedot, M. (2016). Protein-Mediated Precipitation of Calcium Carbonate. *Materials, 9*(11), 944. https://doi.org/10.3390/ma9110944

Postma, P. R., Cerezo-Chinarro, O., Akkerman, R. J., Olivieri, G., Wijffels, R. H., Brandenburg, W. A., & Eppink, M. H. M. (2017). Biorefinery of the macroalgae Ulva lactuca: extraction of proteins and carbohydrates by mild disintegration. *Journal of Applied Phycology, 30*(2), 1281–1293. https://doi.org/10.1007/S10811-017-1319-8

Pramono, H., Pujiastuti, D. Y., & Sahidu, A. M. (2018). Biochemical and physicochemical analysis of fish protein isolate recovered from red snapper (Lutjanus sp.) by-product using isoelectric solubilization/precipitation method. *IOP Conference Series: Earth and Environmental Science, 137*(1), Article 012061. https://doi.org/10.1088/1755-1315/137/1/012061

Prieto, P., Pineda, M., & Aguilar, M. (1999). Spectrophotometric Quantitation of Antioxidant Capacity through the Formation of a Phosphomolybdenum Complex: Specific Application to the Determination of Vitamin E. *Analytical Biochemistry, 269*(2), 337–341. https://doi.org/10.1006/ABIO.1999.4019

Qi, H., Zhao, T., Zhang, Q., Li, Z., Zhao, Z., & Xing, R. (2005). Antioxidant activity of different molecular weight sulfated polysaccharides from Ulva pertusa Kjellm (Chlorophyta). *Journal of Applied Phycology, 17*(6), 527–534. https://doi.org/10.1007/s10811-005-9003-9

Rashad, S., El-Chaghaby, G., Lima, & E. C., Simoes, G., & Reis, D. (n.d.). *Optimizing the ultrasonic-assisted extraction of antioxidants from Ulva lactuca algal biomass using factorial design*. doi:10.1007/s13399-021-01516-8.

Rodrigues, D., Sousa, S., Silva, A., Amorim, M., Pereira, L., Rocha-Santos, T. A. P., … Freitas, A. C. (2015). Impact of enzyme- and ultrasound-assisted extraction methods on biological properties of red, brown, and green seaweeds from the Central West Coast of Portugal. *Journal of Agricultural and Food Chemistry, 63*(12), 3177–3188. https://doi.org/10.1021/jf504220e

Romero, A., Bengoechea, C., Cordobés, F., & Guerrero, A. (2009). Application of thermal treatments to enhance gel strength and stability of highly concentrated crayfish-based emulsions. *Food Hydrocolloids, 23*(8), 2346–2353. https://doi.org/10.1016/j.foodhyd.2009.06.012

Schröder, A., Berton-Carabin, C., Venema, P., & Cornacchia, L. (2017). Interfacial properties of whey protein and whey protein hydrolysates and their influence on O/W emulsion stability. *Food Hydrocolloids, 73*, 129–140. https://doi.org/10.1016/j.foodhyd.2017.06.001

Soria, A. C., & Villamiel, M. (2010). Effect of ultrasound on the technological properties and bioactivity of food: A review. Issue 7. In *Trends in Food Science and Technology* (pp. 323–331). Elsevier. https://doi.org/10.1016/j.tifs.2010.04.003.

Sun, Y., Chen, J., Zhang, S., Li, H., Lu, J., Liu, L., … Jiaping, L. (2014). Effect of power ultrasound pre-treatment on the physical and functional properties of reconstituted milk protein concentrate. *Journal of Food Engineering, 124*, 11–18. https://doi.org/10.1016/j.jfoodeng.2013.09.013

Tian, J., Wang, Y., Zhu, Z., Zeng, Q., & Xin, M. (2015). Recovery of Tilapia (Oreochromis niloticus) Protein Isolate by High-Intensity Ultrasound-Aided Alkaline Isoelectric Solubilization/Precipitation Process. *Food and Bioprocess Technology, 8*(4), 758–769. https://doi.org/10.1007/s11947-014-1431-6

Timilsena, Y. P., Adhikari, R., Barrow, C. J., & Adhikari, B. (2016). Physicochemical and functional properties of protein isolate produced from Australian chia seeds. *Food Chemistry, 212*, 648–656. https://doi.org/10.1016/j.foodchem.2016.06.017

Tullberg, C., Larsson, K., Carlsson, N. G., Comi, I., Scheers, N., Vegarud, G., & Undeland, I. (2016). Formation of reactive aldehydes (MDA, HHE, HNE) during the digestion of cod liver oil: Comparison of human and porcine in vitro digestion models. *Food and Function, 7*(3), 1401–1412. https://doi.org/10.1039/c5fo01332a

Undeland, I., Hall, G., Wendin, K., Gangby, I., Rutgersson, A., Undeland, I., … Rutgersson, A. (2005). Preventing lipid oxidation during recovery of functional proteins from herring (Clupea harengus) fillets by an acid solubilization process. *Journal of Agricultural and Food Chemistry, 53*(14), 5625–5634. https://doi.org/10.1021/jf0404445

Villamonte, G., Pottier, L., & de Lamballerie, M. (2015). Influence of high-pressure processing on the physicochemical and the emulsifying properties of sarcoplasmic proteins from hake (Merluccius merluccius). *European Food Research and Technology, 242*(5), 667–675. https://doi.org/10.1007/S00217-015-2574-Z

Wagner, J. R., Sorgentini, D. A., & Anon, M. C. (2000). Relation between solubility and surface hydrophobicity as an indicator of modifications during preparation processes of commercial and laboratory-prepared soy protein isolates. *Journal of Agricultural and Food Chemistry, 48*(8), 3159–3165. https://doi.org/10.1021/jf990823b

Westphalen, A. D., Briggs, J. L., & Lonergan, S. M. (2006). Influence of muscle type on rheological properties of porcine myofibrillar protein during heat-induced gelation. *Meat Science, 72*(4), 697–703. https://doi.org/10.1016/j.meatsci.2005.09.021

Wu, H., Abdollahi, M., & Undeland, I. (2021). Effect of recovery technique, antioxidant addition and compositional features on lipid oxidation in protein enriched products from cod- salmon and herring backbones. *Food Chemistry, 360*, Article 129973. https://doi.org/10.1016/j.foodchem.2021.129973

Yin, T., He, Y., Liu, L., Shi, L., Xiong, S., You, J., … Huang, Q. (2019). Structural and biochemical properties of silver carp surimi as affected by comminution method. *Food Chemistry, 287*, 85–92. https://doi.org/10.1016/j.foodchem.2019.02.066

Zhang, J., Abdollahi, M., Alminger, M., & Undeland, I. (2022). Cross-processing herring and salmon co-products with agricultural and marine side-streams or seaweeds produces protein isolates more stable towards lipid oxidation. *Food Chemistry, 382*, Article 132314. https://doi.org/10.1016/j.foodchem.2022.132314

Zhou, L., Feng, X., Yang, Y., Chen, Y., Wang, J., Wei, S., & Li, S. (2019). Effects of high-speed shear homogenization on properties and structure of the chicken myofibrillar protein and low-fat mixed gel. *LWT, 110*, 19–24. https://doi.org/10.1016/j.lwt.2019.04.061